The Astrophysical Journal, 698:1010–1019, 2009 June 20 doi:10.1088/0004-637X/698/2/1010
© 2009. The American Astronomical Society. All rights reserved. Printed in the U.S.A.

HIGH-REDSHIFT METALS. I. THE DECLINE OF C IV AT $z > 5.3$*

George D. Becker[1,2], Michael Rauch[2], and Wallace L. W. Sargent[3]
[1] Fellow, Kavli Institute for Cosmology and Institute of Astronomy, Madingley Road, Cambridge CB3 0HA, UK; gdb@ast.cam.ac.uk
[2] Carnegie Observatories, 813 Santa Barbara Street, Pasadena, CA 91101, USA; mr@ociw.edu
[3] Palomar Observatory, California Institute of Technology, Pasadena, CA 91125, USA; wws@astro.caltech.edu
Received 2008 December 11; accepted 2009 April 3; published 2009 May 27

ABSTRACT

We present the results from our search for C IV absorption systems at redshifts $z = 5.3$–6.0. We have observed four $z \sim 6$ QSOs with Keck/NIRSPEC in echelle mode. The data are the most sensitive yet taken to search for C IV at these redshifts, being 50% complete at column densities $\log N_{\rm C\,IV} \approx 13.4$ (cm^{-2}). We find no clear C IV systems in any of the four sight lines. Taking into account our completeness, this translates into a decline in the number density of C IV absorbers in the range $13.2 < \log N_{\rm C\,IV} < 15.0$ of at least a factor ~4.1 (95% confidence) from $z \sim 2$–4.5, over which the number density is relatively constant. We use our lack of detections, along with results from previous studies, to set limits on the slope and normalization of the column density distribution at $z = 5.3$–6.0. The rapid evolution of C IV at these redshifts suggests that the decrease in the number density may largely be due to ionization effects, in which case many of the metals in the $z \sim 4.5$ intergalactic medium (IGM) could already be in place at $z \sim 5.3$, but in lower ionization states. The lack of weak systems in our data, combined with the presence of strong C IV absorbers along at least one other sight line, further suggests that there may be large-scale variations in the enrichment and/or ionization state of the $z \sim 6$ IGM. Alternatively, the known C IV absorbers at these redshifts may not reside in the general IGM, but may be associated with rare, UV-bright star-forming galaxies.

Key words: cosmology: observations – early universe – intergalactic medium – quasars: absorption lines

Online-only material: color figures

1. INTRODUCTION

Metal absorption lines are one of our most versatile tools for studying the high-redshift universe. Just as the ionization history of the intergalactic medium (IGM) reflects the output of ionizing photons from star-forming galaxies and quasars, the metal content of the IGM can be used to infer the integrated and instantaneous rates of global star formation. At very high redshifts, where the direct detection of galaxies becomes increasingly challenging, metal absorption lines can serve as sign posts to the "typical" galaxies that may be responsible for reionizing the universe at $z > 6$. Perhaps, most intriguingly, metal lines can also serve as a probe of the reionization process itself.

A considerable amount of work on the high-redshift universe has focused on cosmic reionization, yet the timing and mechanisms by which the IGM becomes permanently ionized remain poorly understood. The three main observational constraints on reionization are (1) the electron optical depth measured from the polarization of the cosmic microwave background (CMB), (2) the evolution of the high-redshift Lyα forest, and (3) the luminosity functions of high-redshift Lyα-emitting galaxies (LAEs). Five-year *Wilkinson Microwave Anisotropy Probe (WMAP)* measurements of the CMB are consistent with an instantaneous reionization at $z_r \sim 11$, but are also compatible with an extended reionization process (Dunkley et al. 2009). The rapid evolution of the mean transmitted Lyα flux in the spectra of $z \gtrsim 5.7$ quasars has been used to infer that hydrogen reionization may have ended as recently as $z \sim 6$ (Becker et al. 2001; White et al. 2003; Fan et al. 2002, 2006; Gnedin & Fan 2006). The quasar results remain controversial, however (e.g., Songaila 2004; Oh & Furlanetto 2005; Lidz et al. 2006; Becker et al. 2007). Lyα saturates for even a tiny neutral fraction ($f^V_{\rm H\,I} \sim 10^{-3}$; Fan et al. 2002), making it extremely challenging to measure the ionization state of the IGM at these redshifts directly from the Lyα forest. Finally, the lack of a sharp decline in the luminosity function of LAEs from $z \approx 5.7$ to $z \approx 6.5$ suggests that most of the volume of the IGM is already highly ionized by $z \sim 6.5$. (e.g., Malhotra & Rhoads 2004, 2006; Hu & Cowie 2006; Dijkstra et al. 2007, but see Kashikawa et al. 2006). Interpreting the LAE results is somewhat complicated, however, as Lyα photons may escape through locally ionized bubbles (e.g., Haiman & Cen 2005; Wyithe & Loeb 2005; Furlanetto et al. 2006) or by redshifting via galactic winds before passing through the IGM (Santos 2004).

Quasar metal absorption lines provide a complimentary tool for studying the ionization state of the IGM. In a reionization scenario where galaxies provide most of the ionizing flux, overdense regions of the IGM should be the first to become enriched, yet may remain significantly neutral until the end of reionization due to the short recombination times at high densities. "Forests" of low-ionization absorption lines such as O Iλ1302, Si IIλ1260, and C IIλ1334 may therefore be present prior to the completion of reionization (Oh 2002). Our recent search for O I using Keck/HIRES spectra of $z > 5$ QSOs yielded mixed results (Becker et al. 2006). While an overdensity of low-ionization absorbers at $z \sim 6$ was found along at least one sight line, SDSS J1148+5251 ($z_{\rm Q} = 6.42$), no enhancement was seen toward SDSS J1030+0524 ($z_{\rm Q} = 6.30$), which has a complete Gunn–Peterson trough spanning ~80 comoving Mpc (White et al. 2003). These differences suggest there may be large-scale variations in the enrichment and/or ionization state of the IGM at $z \sim 6$, and perhaps a strong redshift evolution in the ionization state of metal absorption systems. The

* The observations were made at the W.M. Keck Observatory which is operated as a scientific partnership between the California Institute of Technology and the University of California; it was made possible by the generous support of the W.M. Keck Foundation.

metal-enriched, low-ionization regions toward SDSS J1148+5251 may represent the final stages of reionization. Alternatively, they may arise by chance from multiple pockets of enriched gas near galaxies aligned along a filament.

In order to effectively use metal lines as probes of reionization, the roles of enrichment and ionization must be separately understood. A quasar sight line that passes through a largely neutral IGM may not show an O I forest if the IGM has not yet been enriched. At lower redshifts, highly ionized species such as C IV and Si IV have been the primary tracers of IGM metallicity (e.g., Meyer & York 1987; Sargent et al. 1988; Petitjean & Bergeron 1994; Cowie et al. 1995; Ellison et al. 1999; Schaye et al. 2003; Pettini et al. 2003; Aguirre et al. 2004; Simcoe et al. 2004; Scannapieco et al. 2006). Both the comoving mass density and the column density distribution of C IV remain roughly constant over at least $1.5 \lesssim z \lesssim 4.5$ (Songaila 2001). Since the fraction of carbon in the form of C IV varies depending on the ionization state of the gas, however, a constant C IV density does not necessarily mean that the total IGM metallicity remains unchanged (e.g., Oppenheimer & Davé 2006). Nevertheless, some fraction of IGM metals are clearly in place by $z \sim 4.5$.

The current constraints on the abundance of metals in the IGM at $z > 5$ are mixed. Songaila (2005) found tentative evidence for a decrease in the comoving mass density of C IV from $z \sim 4$ to 5. To measure the metal content of the IGM at even higher redshifts the C IVλ1548, 1551 doublet must be pursued into the near infrared. Preliminary searches by Simcoe (2006) and Ryan-Weber et al. (2006) found evidence for a comoving C IV mass density at $z \sim 6$ that is consistent with measurements at $z \sim 2$–4.5. In addition, Simcoe (2006) found tentative evidence that the C IV column density distribution may also remain constant out to $z \sim 6$. These works examined only two sight lines, however, and were generally sensitive only to the rare, high column density ($\log N_{\rm C\,IV} \gtrsim 13.8$) systems that dominate the comoving mass density. A complete census of C IV at $z \sim 6$ requires a broader, more sensitive search.

In this series of papers, we present the results from a two-part search for intergalactic metals at $z \sim 6$. In this paper, we describe our survey for C IV performed with Keck/NIRSPEC in high-resolution mode. This is the most sensitive search for C IV at $z > 5.3$ yet performed, partly due to the high resolution ($R \approx 13,000$), which is better suited to search for narrow ($b \sim 10$ km s^{-1}, Rauch et al. 1996) lines than previous studies. By covering multiple sight lines with high sensitivity, we are able to place strong constraints on the abundance of the kinds of highly ionized absorbers that are common at lower redshifts. In the following paper, we will expand our search for low-ionization systems initially presented in Becker et al. (2006). The combined results will provide unique constrains not only on the ionization state of the IGM, but on the star-formation history of the universe at $z > 5$.

The rest of the paper is organized as follows. The data are presented in Section 2. In Section 3 we give the results of our search for C IV, along with our completeness estimates. We show that the number density of C IV absorbers at $z > 5.3$ has declined sharply from $z \sim 2$–4.5 in Section 4, and give constraints on the column density distribution and the contribution of C IV to the closure density. In Section 5, we discuss possible reasons for the decrease in C IV with redshift and the significance of our lack of detections in light of the strong systems previously reported along other sight lines. Finally, our conclusions are presented in Section 6. Throughout this paper, we assume $\Omega_{\rm m} = 0.274$, $\Omega_\Lambda = 0.726$, and $H_0 = 70.5$ km s^{-1} (Komatsu et al. 2009).

Table 1
Summary of NIRSPEC Echelle Observations

QSO[a]	Redshift	$t_{\rm exp}$ (hr)	S/N[b]	$\Delta z_{\rm C\,IV}$[c]	$\Delta X_{\rm C\,IV}$[d]
SDSS J0002+2550	5.82	12.0	11.4–16.7	0.458	2.33
SDSS J0818+1722	6.00	11.0	10.3–14.2	0.638	3.29
SDSS J0836+0054	5.80	11.5	14.5–21.5	0.438	2.23
SDSS J1148+5251	6.42	12.0	10.9–15.6	0.679	3.44

Notes.
[a] QSO names given as SDSS Jhhmm+ddmm.
[b] Middle 50% range of signal-to-noise ratio per resolution element values for pixels within the wavelength interval used to search for C IV.
[c] Total redshift interval used to search for C IV.
[d] Total absorption path-length interval used to search for C IV.

2. THE DATA

2.1. NIRSPEC Echelle Spectra

We obtained high-resolution, near-IR spectra of four $z \sim 6$ QSOs with Keck/NIRSPEC (McLean et al. 1998) between February 2007 and February 2008. The spectrograph was used in echelle mode in the NIRSPEC-1 (Y) band, which provides continuous wavelength coverage over $\lambda \approx 0.95$–1.13 μm in a single setting. Our observations are summarized in Table 1. Individual exposures were 1800 s, with total integration times of 11–12 hr per object.

Data reduction was performed using a custom set of IDL routines tailored to the technical challenges of observing faint targets in the infrared. The NIRSPEC detector, a 1024 × 1024 ALLADIN-3 InSb array, has good sensitivity in the near infrared but also a high dark current. The sky emission lines are widely separated in echelle mode, leaving the dark current as the dominant source of noise, provided that other sources such as variable bias levels, hot pixels, and numerous cosmetic blemishes can be properly removed.

Rather than nod-subtract our exposures, which automatically multiplies the noise from the sky and the dark current by a factor of root 2, we compiled a low-noise dark frame by taking a large set of dark exposures with the same exposure time as our science frames. This was used to remove dark current features and other blemishes prior to sky subtraction. The exposures were flat fielded using internal flats. In order to correct for pixel-to-pixel variations separately from the high-frequency fringing introduced by interference between the order sorting and blocking filters, the fringe pattern was modeled and removed from the two-dimensional flats. Each science exposure was then divided by the "pixel" flat, as well as by the fringe model after it was scaled in intensity and shifted on the detector to match the exposure.

The sky was modeled using a b-spline fit and removed from each exposure using optimal sky subtraction techniques (Kelson 2003). The residual bias level from each of the 32 independent readout channels was modeled and removed both at the start of the reduction and again after a first-pass sky subtraction. Similar care was taken to remove the residual bias in the dark frames.

In order to maximize the signal-to-noise ratios of the final spectra, we performed optimal spectral extraction simultaneously on all exposures for a given object. The object spatial profile was modeled independently for each exposure. A response function derived from a standard star exposure was also

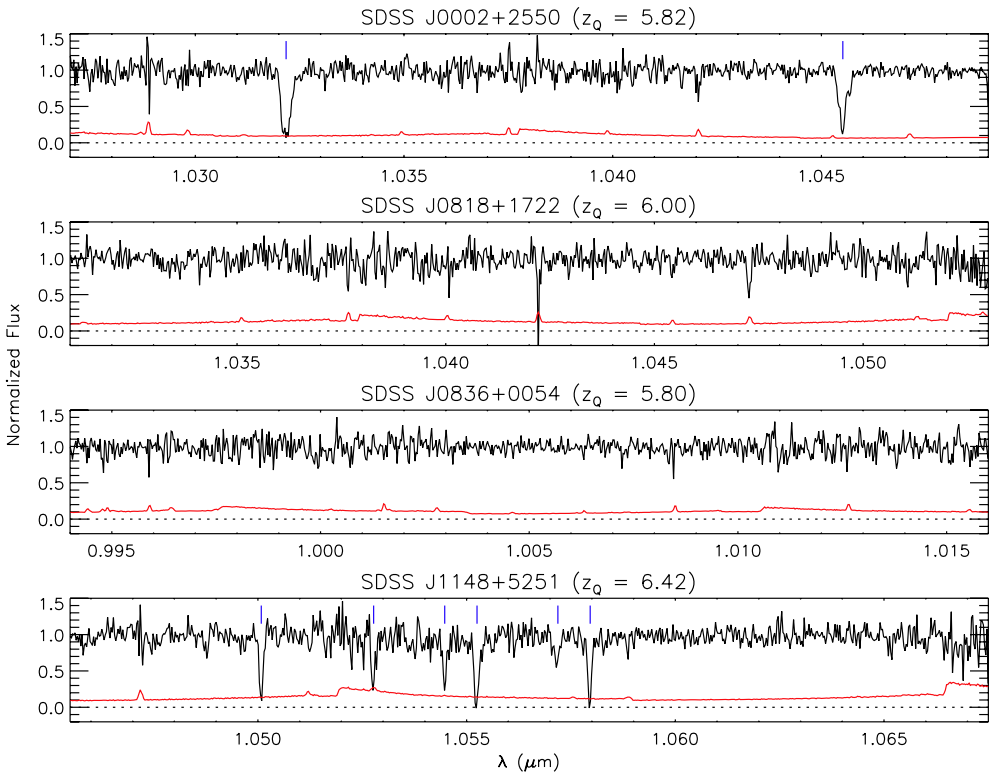

Figure 1. Example sections of the final one-dimensional normalized NIRSPEC echelle spectra. The formal error arrays are shown in red. Genuine absorption lines are identified with tick marks. The lines in the spectrum of SDSS J0002+2550 are Fe II λ2344, 2374 at $z = 3.404$. Those in the spectrum of SDSS J1148+5251 are three sets of Mg II λ2796, 2804 doublets at $z \approx 2.77$. Features in the flux that coincide with spikes in the error arrays are typically residuals from the subtraction of strong skylines.

(A color version of this figure is available in the online journal.)

applied to the counts in the two-dimensional frames. A single one-dimensional spectrum was then extracted from all exposures of a given object simultaneously using optimal weighting (Horne 1986). This technique allowed us to best reject spurious pixels while preserving as much information as possible from the two-dimensional arrays, which were individually very noisy even after careful reduction. The one-dimensional spectra were then normalized using a slowly varying spline fit to the continuum. Telluric absorption correction was done using a model of the atmospheric transmission in the *Y* band (Hinkle et al. 2003). This produced better results than using our standard star spectra, which contained some residual high-frequency ringing as a result of the fringing. Even so, we have restricted our analysis to the center of the transmission window (9850–10920 Å), where there is very little atmospheric absorption. Finally, we scaled the formal error arrays so that the distribution of deviations of the flux from the continuum fit, normalized by the error array, was well fitted by a Gaussian distribution with unit variance for each object. The typical resulting increase in the error array was ∼30%, which is a reasonable estimate for the amount of noise that could not be well characterized in the two-dimensional frames.

Representative sections of the final spectra are shown in Figure 1. The data tend to become noisy at the ends of the echelle orders, which are marked by a step in the error array. The measured resolution is $R \approx 13000$ (FWHM ≈ 23 km s^{-1}). Narrow metal lines can clearly be seen, though these are at much lower redshifts. Significantly, the noise properties of the data are well behaved, with a scatter as a function of wavelength that is reasonably well described by the scaled error array. This is essential for correctly estimating our sensitivity.

2.2. Optical Spectra

We have also acquired high-resolution optical spectra of several $z \sim 6$ QSOs, including the four we observed with NIRSPEC. Some of these data were presented in Becker et al. (2006, 2007), and the new observations will be discussed more thoroughly in the next paper. Here we will use Keck HIRES (Vogt et al. 1994) spectra of SDSS J0836+0524 and SDSS J1030+0524 ($z_Q = 6.30$) to help evaluate candidate C IV detections along those sight lines. The data were reduced using a custom IDL pipeline featuring optimal sky subtraction. As with the NIRSPEC data, simultaneous optimal extraction was also used to maximize the signal-to-noise ratio of the final spectra. Prior to extraction, the two-dimensional counts were flux calibrated using a response function generated from a standard star. Telluric absorption correction using a standard star was also applied to the two-dimensional frames. Velocity offsets between the standard and the science frames, as well as variations in the strength of the H_2O and O_2 absorption bands, were determined from preliminary extractions of groups of individual exposures taken near the same time. Since SDSS J1030+0524 was observed on multiple runs at different times of the year, shifts in the relative velocity of the object allowed residuals from atmospheric absorption and emission to be especially well rejected.

3. RESULTS OF C IV SEARCH

We searched for C IV doublets in our NIRSPEC data both by eye and using an automated technique described below. Although the spectra were corrected for telluric absorption, we limited our search to the regions between 9820 Å and 10920 Å

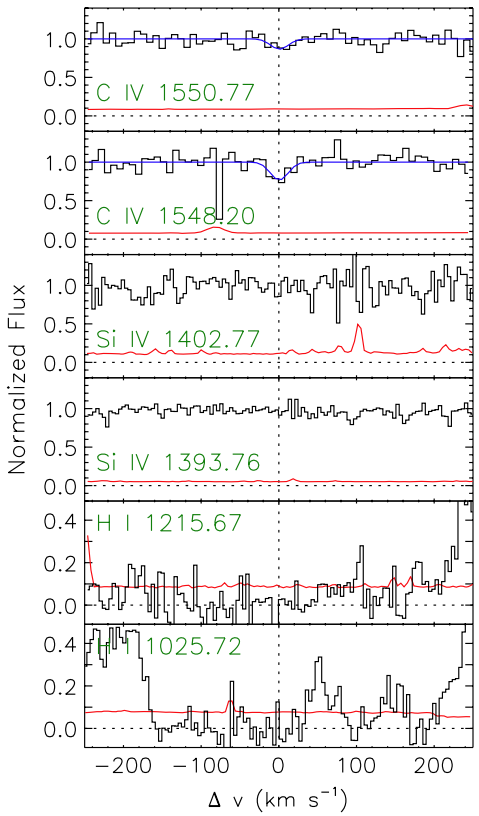

Figure 2. Candidate C IV system at $z = 5.4073$ toward SDSS J0836+0054. Histograms show the normalized flux, which is from NIRSPEC for C IV and HIRES (binned to 4.2 km s^{-1} for display) for Si IV and H I. The red lines are the formal error arrays. The blue line is a Voigt profile fit to the candidate C IV absorption, with $N_{\rm C\,IV} = 10^{13.06}$ cm^{-2}. The reality of this system is unclear, as the λ1551 transition is difficult to distinguish from the noise (see text).

(A color version of this figure is available in the online journal.)

($5.34 \leqslant z_{\rm C\,IV} \leqslant 6.04$), which is largely free of atmospheric absorption. The total redshift interval along each sight line is given in Table 1. In cases where the QSO C IV emission line fell in the bandpass, we included the entire region blueward of the line center. While it is customary to exclude a narrow region near the QSO redshift in order to avoid proximity effects, this region is also typically enhanced with C IV absorbers (e.g., Vestergaard 2003; Nestor et al. 2008). Our conclusions below are therefore most likely enhanced by including it in our analysis. In any case, the proximity region comprises only a small part (∼10%) of the total path length toward two of our four QSOs.

Both the manual search and the follow-up automated search revealed only a single candidate C IV absorber, which is at $z = 5.4073$ toward SDSS J0836+0054. This system is plotted in Figure 2. Voigt profile fitting produced a best-fit column density $\log N = 13.06 \pm 0.12$ (cm^{-2}), and a Doppler parameter $b = 5.8 \pm 6.4$ km s^{-1} (i.e., unresolved). Although it was detected by the automatic search algorithm, the depth of the λ1551 transition is consistent with the local noise amplitude. It is not clear, therefore, whether this absorber is real. Using the HIRES spectrum of SDSS J0836+0054, we can inspect the Si IV and H I Lyα and Lyβ absorption at the same redshift. The H I Lyα and Lyβ appear saturated, which is consistent with it being a real absorption system. There is no detectable Si IV. While this does not rule out a genuine C IV absorber, it means that we cannot independently confirm that the system is legitimate. Verification of this absorber will therefore require near-IR data of significantly higher quality.

3.1. Completeness

To assess the significance of our lack of C IV detections we have estimated our completeness as a function of column density using a Monte Carlo method. Artificial C IV doublets were inserted randomly into the data and an automated algorithm was used to determine whether these systems could be detected. We generated 10^4 doublets for each sight line, ranging in column density from 10^{12} to 10^{15} cm^{-2}. Doppler parameters were selected from the measured distribution of Rauch et al. (1996).

In order to be considered a detection, we first required the flux decrement to exceed the local error at the wavelength of both lines of the doublet after the spectra were smoothed by the instrumental resolution (FWHM = 23 km s^{-1}). We then fitted independent Gaussians to each line (using the unsmoothed data), and evaluated the reliability of the fits and the agreement between the two lines. Our tolerances were stricter for the stronger λ1548 transition. For a satisfactory fit, the redshift uncertainty was required to be less than 0.5 (1.0) times the resolution for the λ1548 (λ1551) transition. We further required that the fitted flux decrement be greater than 3.0 (2.0) times the fit uncertainty, and that the line width be greater than both 3.0 (1.0) times the fit uncertainty and 0.5 times the resolution. A "detection" was only counted when the line fits were also consistent with being a doublet. In order to exclude potential false positives, we set stricter requirements for weaker systems, since strong systems are typically easy to identify by eye. When the peak optical depth of the λ1548 transition was less (greater) than 1.0, we required that the velocity offset between the two fits be less than both 1.0 (2.0) times the resolution and 2.0 (3.0) time the combined uncertainty in the fitted velocities. The line widths were required to agree to within half the width of the narrower line, or three times the combined uncertainty. In all cases, however, the line widths could not disagree by more than a factor of 2. Finally, if the peak optical depth of one or both lines was less than 1, we required the ratio of the optical depths $\tau^{\rm peak}_{\lambda1548}/\tau^{\rm peak}_{\lambda1551}$ to be between 0.8 and 3.0.

Defining criteria for an automated search is a somewhat subjective process, as selection thresholds and goodness-of-fit requirements will vary depending on the line-fitting method. The above procedure was designed to give the same result as a visual evaluation of the synthetic lines as often as possible. In general, this meant applying greater scrutiny to weaker systems in order to avoid false positives. We found very good agreement overall between the fraction of systems identified by eye and by the automated method.

Our completeness results are shown in Figure 3. We are most complete at $\log N_{\rm C\,IV} > 13.7$, though we are still ∼50% complete in the full sample at $\log N_{\rm C\,IV} = 13.4$, and ∼20% complete at $\log N_{\rm C\,IV} = 13.2$. As discussed below, the fact that we are significantly complete over a wide range of column densities allows us to put strong constraints on the column density distribution of C IV absorbers.

3.2. False Detection Rate

Even for a carefully designed search algorithm, contamination by false positive detections can be a significant issue when the total number of detections is near zero. We have attempted to characterize the noise properties of our data as accurately as possible, which is a significant challenge when working with an InSb detector at low flux levels. Even so, some false detections may occur if there is additional, uncharacterized noise, such as from fringing that has not been fully corrected, the residuals of

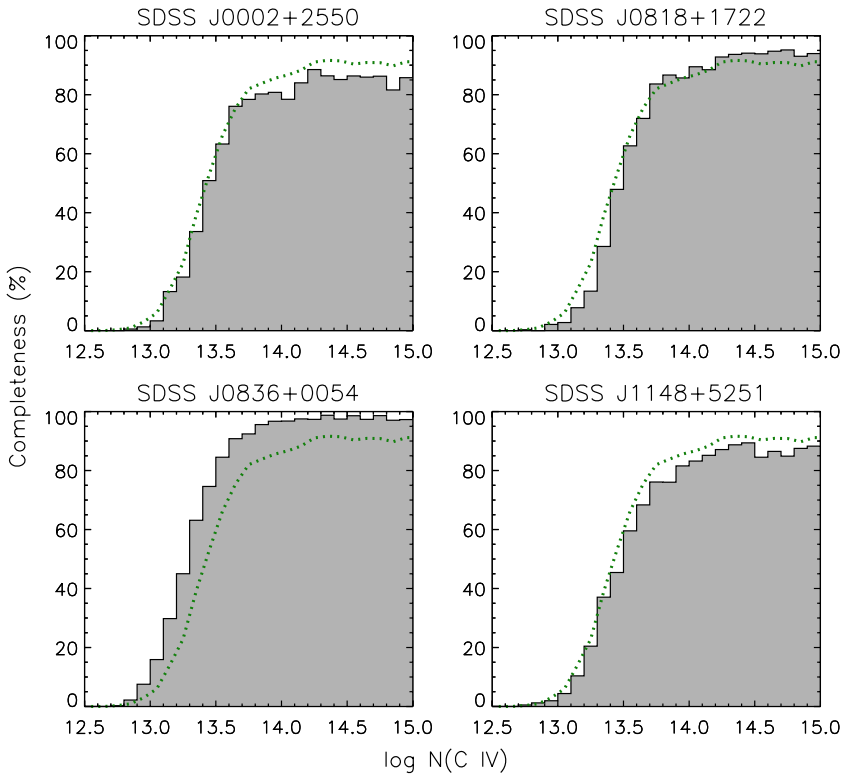

Figure 3. Percentage of recovered artificial C IV doublets as a function of column density. Histograms give the completeness for individual sight lines. The dotted line is the path-length-weighted mean for the entire sample. The completeness does not go to 100% for large column densities because of the non-negligible chance that of one of the C IV components may coincide with a lower-redshift absorption line, the residual from a subtracted skyline, or some other unusable part of the spectrum. The completeness for SDSS J0836+0054 is higher partly because there are fewer lower-redshift lines along that sight line.

strong skylines, or errors in the subtraction of patterned read noise. Chance superpositions of unrelated absorption lines can also generate false detections, although such cases can generally, though not always, be recognized.

In order to estimate the number of false positive detections we would expect, we employed the same automated method to search the data for "fake" C IV doublets whose velocity separation is offset from the true C IV doublet separation. In each trial, we adjusted the doublet separation by twice the instrumental resolution, omitting separations that were similar to true doublets such as Mg IIλ2796, 2804, or other plausible combinations of intervening absorption lines. In 20 trials, we detected seven false doublets. This gives an expectation value of 0.35, or a 30% chance of finding one or more false positives in our data set. This rate is consistent with the candidate system at $z = 5.4073$ toward SDSS J0836+0524 being a false detection.

To limit potential contamination from false positives, we have restricted our analysis below to column densities $\log N_{\rm C\,IV} > 13.2$. Above this limit, there are regions in the data where the depth of both doublet transitions would clearly exceed the local noise amplitude, permitting more secure identification of genuine C IV systems. We are formally sensitive down to $\log N_{\rm C\,IV} \sim 13.0$, but a small number of real detections at this level would be difficult to distinguish from a small number of false positives. We therefore use a more conservative cutoff in column density.

4. CONSTRAINTS ON C IV IN THE $Z \sim 6$ IGM

4.1. Change in the Number Density of Absorbers from $z \sim 3$

We can use our completeness estimates to calculate the number of detections we should expect if the column density distribution has not evolved from lower redshifts. It is conventional to fit a power law of the form

$$f(N_{\rm C\,IV}) \equiv \frac{\partial^2 \mathcal{N}}{\partial N_{\rm C\,IV}\, \partial X} = B \left(\frac{N_{\rm C\,IV}}{N_0} \right)^{-\alpha}. \quad (1)$$

Here, X is the absorption path-length interval, defined such that, for a nonevolving population of sources, $d\mathcal{N}/dX$ remains constant with redshift. For $\Omega = 1$,

$$\frac{dX}{dz} = \frac{(1+z)^2}{\sqrt{\Omega_{\rm m}(1+z)^3 + \Omega_\Lambda}}. \quad (2)$$

Fitting a large sample of absorbers at $z = 2.90$–3.54, Songaila (2001) found a slope $\alpha = 1.8 \pm 0.1$ for systems with $\log N_{\rm C\,IV} > 13.0$, with a normalization $B = 10^{-12.67}$ (corrected for our adopted cosmology) at $N_0 = 10^{13.0}$ cm^{-2}. Indeed, they found that this distribution is nearly invariant out to at least $z \approx 4.5$. Songaila (2005) found a slightly shallower slope ($\alpha = 1.7$) and a higher normalization when fitting the distribution of "pseudoclouds" identified by an automated method. We will compare our results to the Songaila (2001) fit, however, since the search method is more similar to the one used here.

Figure 4 shows our mean completeness function convolved with the column density distribution of Songaila (2001). We would expect the largest number of detections near $\log N_{\rm C\,IV} \sim 13.5$, but there are significant tails toward both ends of the column density range. In total, we would expect to detect 12.3 systems with $\log N_{\rm C\,IV}$ between 13.2 and 15.0 along all four sight lines if $f(N_{\rm C\,IV})$ was unchanged from $z \sim 3$. For zero detections, the 95% and 99% one-sided confidence limits on the mean expected number are 3.0 and 4.6, respectively, assuming

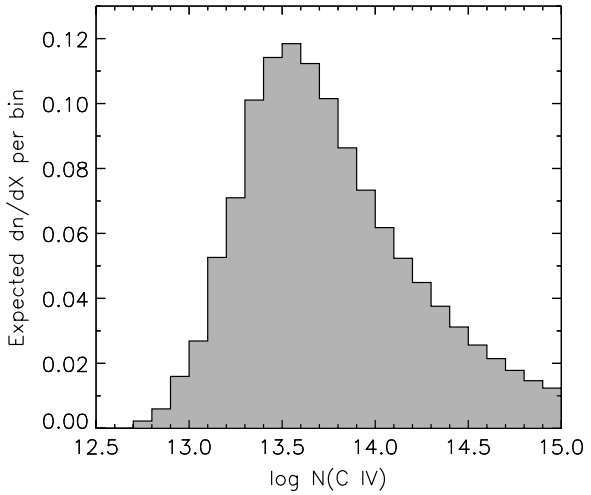

Figure 4. Expected C IV detection rate for a column density distribution that is unchanged from $z \sim 2$–4.5. We computed the expected number of C IV systems per unit redshift path interval per 0.1 dex column density bin by integrating $f(N_{\rm C\,IV})$ from Songaila (2001) against our path-length-weighted mean completeness (Figure 3). Over our entire sample, we would expect to detect 12.3 systems with $13.2 \leqslant \log N_{\rm C\,IV} \leqslant 15.0$.

Poisson statistics (e.g., Gehrels 1986). This translates into a 95% confidence limit of at least a factor of 4.1 decline in the number density of C IV systems from $z \sim 3$ to $z = 5.3$–6.0, or a 99% limit of a factor of 2.7. We note that with the Songaila (2005) $f(N_{\rm C\,IV})$ we would have expected 20 systems. Similarly, using $f(N_{\rm C\,IV})$ from a fit to the C IV distribution in nine high-quality HIRES spectra from Boksenberg et al. (2003), we would have expected 16 lines. Adopting the Songaila (2001) column density distribution may therefore be somewhat conservative.

4.2. Previously Studied Sight Lines

Given the large drop in the number density of absorbers we observe, it is worth reviewing the results from the initial searches for C IV at $z > 5.3$. Simcoe (2006) obtained Gemini/GNIRS spectra of two $z \sim 6$ QSOs, SDSS J1306+0356 ($z_Q = 6.00$) and SDSS J1030+0524 ($z_Q = 6.27$). Ryan-Weber et al. (2006) observed the same two QSOs with VLT/ISAAC, though only obtained usable data for SDSS J1030+0524. Simcoe found a number of low-column density absorbers along both sight lines. As the author points out, however, the majority of these detections are near the detection limit and are consistent with the expected number of false detections. They found at least one secure absorber, which occurs toward SDSS J1030+0524 at $z = 5.829$ with $\log N_{\rm C\,IV}^{\rm total} = 13.8$. Ryan-Weber et al. also detected this system, albeit marginally (they measure a much higher column density, but this may be due to blending of the λ1551 transition with an unrelated line that is visible in the GNIRS spectrum). They further detect a system at $z = 5.724$ that is unclear in the GNIRS data. We have checked the authenticity of the $z = 5.724$ system by searching for related lines in our HIRES spectrum of SDSS J1030+0524. The optical data, as presented in Figure 5, show Si IV absorption at the redshift of the candidate C IV. We confirm the large ($\sim$60 km s^{-1}) velocity width measured by Ryan-Weber et al. (2006). At HIRES resolution, the Si IV absorption is clearly asymmetric and best fitted using multiple components (see Table 2). Assuming that the C IV absorption has the same kinematic structure and relative component strength as the Si IV, we were able to roughly reproduce the equivalent width of the

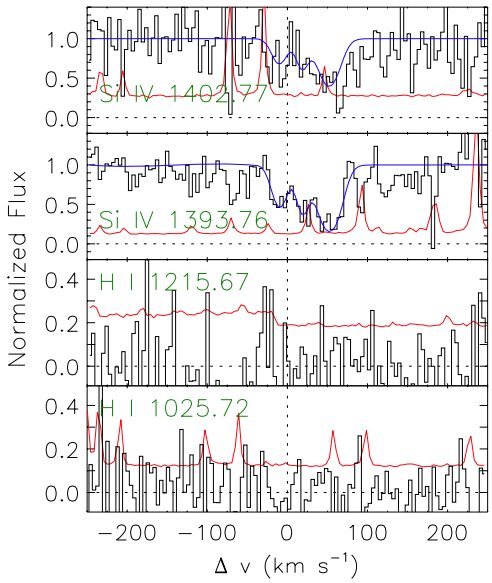

Figure 5. HIRES data showing the Si IV and H I absorption profiles for the candidate C IV system at $z = 5.724$ toward SDSS J1030+0524 (Ryan-Weber et al. 2006). The spectrum has been binned using 4.2 km s^{-1} pixels for display. The blue line is a Voigt profile fit to the Si IV using three components (Table 2). While the data are too noisy to determine the exact kinematic structure, the Si IV is apparently not saturated, and therefore the total fitted column density does not change significantly when more components are added.

(A color version of this figure is available in the online journal.)

Table 2
Voigt Profile Fit to Si IV at $z = 5.724$ Toward SDSS J1030+0524

z	b (km s^{-1})	$\log N$(cm^{-2})
5.7235623 ± 0.000049	11.8 ± 3.6	12.97 ± 0.10
5.7242061 ± 0.000063	9.2 ± 4.2	12.98 ± 0.17
5.7249523 ± 0.000042	16.2 ± 2.7	13.47 ± 0.06

Notes. These are the best-fitting parameters for a three component fit to Si IV in the HIRES data. Increasing the number of components does not significantly change the total column density.

Ryan-Weber et al. fit using a total C IV column density very similar to their measured $\log N_{\rm civ} = 14.4$. Thus, there do not seem to be any hidden saturation effects in the ISAAC data.

In summary, in the two sight lines studied by Simcoe (2006) and Ryan-Weber et al. (2006) there are two confirmed $z \sim 6$ C IV systems. These lie along a single sight line, and they are both strong ($\log N_{\rm C\,IV} > 13.8$) systems. The weaker candidates reported by Simcoe (2006) are broadly consistent with their expected false positive rate.

4.3. Constraints on the Column Density Distribution

We can set joint constraints on the slope and normalization of a power-law distribution of C IV column densities. For a given slope α, we have calculated the 95% limits on B by adjusting the normalization such that we would expect to detect the Poisson upper limit of 3.0 C IV systems along our four sight lines. In calculating B, we take into account our measured completeness and restrict ourselves to the number of expected systems between $\log N_{\rm C\,IV} = 13.2$ and 15.0, for reasons described in Section 3.2 and below. The results are shown in Figure 6. As stated above, if α remains unchanged from $z \sim 3$, then the normalization must decrease by at least a factor of $\sim$4. Alternatively, $f(N_{\rm C\,IV})$ could steepen (larger α)

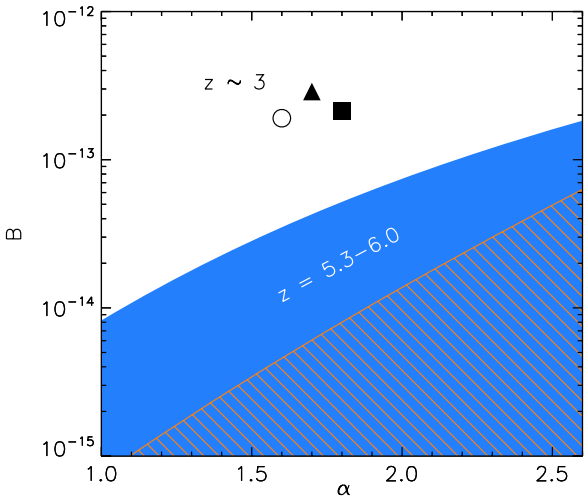

Figure 6. Limits on the column density distribution, $f(N_{\rm C\,IV}) = BN_{\rm C\,IV}^{-\alpha}$, of C IV absorbers at $z = 5.3-6.0$ in the range $13.2 < \log N_{\rm C\,IV} < 15.0$. The solid shaded regions show the range of normalizations allowed at the 95% confidence level for a given power-law slope based on the lack of detections in our NIRSPEC data. Separately, the line-filled regions are excluded at the 95% level based on the fact that there are at least two known systems with $\log N_{\rm C\,IV} \geqslant 13.8$ along six lines of sight (see text). Symbols show fitted parameters for $f(N_{\rm C\,IV})$ at $z \sim 3$; square: Songaila (2001), triangle: Songaila (2005), circle: Boksenberg et al. (2003).

(A color version of this figure is available in the online journal.)

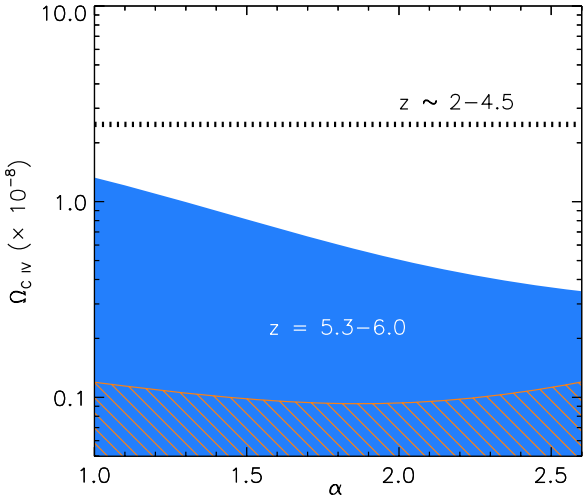

Figure 7. Limits the contribution of C IV to the closure density at $z = 5.3$–6.0, calculated by integrating over the allowed column density distributions in Figure 6. The solid shaded region shows the range of $\Omega_{\rm C\,IV}$ values allowed at the 95% confidence level for a given slope α, based on the lack of detections in our NIRSPEC data. Separately, the line-filled regions are excluded at the 95% level based on the fact that there are at least two known $\log N_{\rm C\,IV} \geqslant 13.8$ systems along six lines of sight. The values for $\Omega_{\rm C\,IV}$ were calculated by integrating Equation (3) over $13.2 < \log N_{\rm C\,IV} < 15.0$ (see the text). The horizontal dotted line shows $\Omega_{\rm C\,IV}$ at $z \sim 2$–4.5 calculated by integrating over the Songaila (2001) $f(N_{\rm C\,IV})$ between the same bounds, which produces good agreement with published observations.

(A color version of this figure is available in the online journal.)

while maintaining a somewhat higher normalization. This would effectively "hide" a greater fraction of the expected systems below our detection limit. It is also possible that $f(N_{\rm C\,IV})$ could become more shallow, shifting the distribution toward stronger lines, provided that the normalization decreases more sharply. In Figure 6, we have only shown the results for $\alpha \geqslant 1$. Formally, α could be less than 1, but this would imply more absorbers per decade in $N_{\rm C\,IV}$ with increasing $N_{\rm C\,IV}$, which is not observed for any other class of absorbers. We further note that low values of α strongly require the assumed high-end cutoff in $N_{\rm C\,IV}$ at $10^{15.0}$ cm^{-2}.

We can further use the detections of Simcoe (2006) and Ryan-Weber et al. (2006) to set lower limits on the normalization of $f(N_{\rm C\,IV})$. The total path length surveyed by those authors and in this work is $\Delta X = 17.4$. For two detections, the one-sided 95% lower limit on the expected mean number is 0.36. In order to set a lower limit on B, we assume 100% completeness and adjust the normalization such that we would expect at least this many systems with $\log N_{\rm C\,IV} = 13.8$–15.0 along all six sight lines. The results are shown in Figure 6. Including this constraint still leaves a significant degeneracy between α and B, but it greatly reduces the range of allowed normalizations for a given power-law slope.

4.4. Limits on $\Omega_{\rm C\,IV}$

Our limits on the total C IV mass density are necessarily weaker than our constraints on $f(N_{\rm C\,IV})$. For $\alpha < 2$, the integrated mass density will be dominated by the highest column density absorbers, which may be too rare to appear in our data. Nevertheless, we can set limits on $\Omega_{\rm C\,IV}$ by integrating over the allowed column density distributions. The contribution of C IV to the closure density ρ_c can be calculated as

$$\Omega_{\rm C\,IV} = \frac{m_{\rm C\,IV}}{\rho_c}\frac{H_0}{c}\int_{N_{\rm min}}^{N_{\rm max}} N_{\rm C\,IV}\, f(N_{\rm C\,IV})\, dN_{\rm C\,IV}\,, \qquad (3)$$

where $m_{\rm C\,IV}$ is the mass of the C IV ion. The choice of integration limits is critical, but there are natural choices for C IV. At lower redshifts, $f(N_{\rm C\,IV})$ tends to become significantly shallower at $\log N_{\rm C\,IV} \lesssim 13$ (e.g., Songaila 2005). Integrating the completeness-corrected fits to $f(N_{\rm C\,IV})$ of Songaila (2005) yields a contribution to $\Omega_{\rm C\,IV}$ below our adopted limit of $10^{13.2}$ cm^{-2} that is < 10% of the contribution between $10^{13.2}$ and $10^{15.0}$ cm^{-2}. At the other end, systems with $\log N_{\rm C\,IV} > 15.0$ are not typically detected, even in large surveys (e.g., Songaila 2001, 2005, but see Scannapieco et al. 2006). There is likely to be another break in the column density distribution above $\log N_{\rm C\,IV} \sim 15.0$, at least at moderate redshifts. Songaila (2001) would have expected to detect ~5 systems with $15 < \log N_{\rm C\,IV} < 16$ between $z = 2.0$ and $z = 4.5$ if their power-law distribution held to these column densities. At $z \sim 2$–4.5, the measured $\Omega_{\rm C\,IV} \sim (2$–$3) \times 10^{-8}$ is well reproduced by integrating over the Songaila (2001) $f(N_{\rm C\,IV})$ between $10^{13.2}$ and $10^{15.0}$ cm^{-2}. We therefore adopt $N_{\rm min} = 10^{13.2}$ cm^{-2} and $N_{\rm max} = 10^{15.0}$ cm^{-2} as our integration limits.

The results of integrating over $f(N_{\rm C\,IV})$ using the allowed values of the power-law slope and normalization are shown in Figure 7. The corresponding value at $z \sim 2$–4.5, obtained by integrating over $f(N_{\rm C\,IV})$ from Songaila (2001), is shown as a horizontal line. Our data demonstrate that $\Omega_{\rm C\,IV}(z = 5.3$–$6.0)$ must be $\lesssim 1.3 \times 10^{-8}$, or $\lesssim 0.5\ \Omega_{\rm C\,IV}(z \sim 2$–$4.5)$. As expected, the largest allowed values of $\Omega_{\rm C\,IV}$ are for very shallow $f(N_{\rm C\,IV})$, which permit there to be rare, strong systems without requiring a large number of weaker systems. If α remains unchanged from $z \sim 2$–4.5, however, then $\Omega_{\rm C\,IV}$ is limited to $\lesssim 6.0 \times 10^{-8}$, or a factor of ~4 less than $\Omega_{\rm C\,IV}(z \sim 2$–$4.5)$. Separately, $\Omega_{\rm C\,IV}(z = 5.3$–$6.0)$ must be $\gtrsim 1 \times 10^{-9}$ in light of the two detected systems toward SDSS J1030+0524. These limits are compared to measurements from the literature in Figure 8. We note that our limits on $\Omega_{\rm C\,IV}$ based on the allowed shape of the

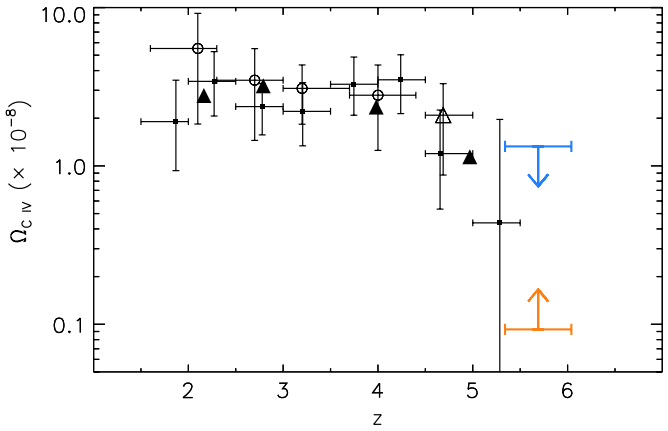

Figure 8. $\Omega_{C\,IV}$ as a function of redshift. The downward-pointing arrow shows the one-sided 95% upper limit on $\Omega_{C\,IV}$ at $z = 5.3$–6.0 set by the lack of detections in our NIRSPEC data (see Figure 7). The limit assumes a power-law column density distribution, $f(N_{C\,IV}) \propto N_{C\,IV}^{\alpha}$, with $\alpha \geqslant 1.0$ for $13.2 < \log N_{C\,IV} < 15.0$. Separately, the upward-pointing arrow shows the 95% lower limit on $\Omega_{C\,IV}$ for $\alpha \geqslant 1.0$ set by the fact that there are at least two known $\log N_{C\,IV} \geqslant 13.8$ systems along six lines of sight. Symbols are measurements from the literature, corrected for our adopted cosmology, with two-sided 90% vertical error bars; small squares: Songaila (2001), filled triangles: Songaila (2005), open circles: Boksenberg et al. (2003), open triangle: Pettini et al. (2003).

(A color version of this figure is available in the online journal.)

column density distribution are consistent with the results from a shallower search for strong C IV systems along a larger number of $z \sim 6$ sight lines (Ryan-Weber et al. 2009).

5. DISCUSSION

Our primary goal in this paper has been to measure the evolution of C IV absorbers at $z = 5.3$–6.0. We have shown that the weak ($\log N_{C\,IV} \gtrsim 13.0$) absorption systems that are ubiquitous at $z < 4.5$ are less abundant by at least a factor of 4 at $z > 5.3$. At face value, this might suggest that the metal content of the IGM is changing rapidly at these redshifts. Several factors, however, must be considered when translating the observed incidence of C IV systems into a global IGM metallicity. The number density of highly ionized metal absorption systems at a given redshift will depend not only on the mean metallicity of the IGM, but also on the spatial distribution of the metals and on the ionization state of the enriched gas. We will have more leverage to assess these factors in a subsequent paper, in which we examine the role of low-ionization metal absorption systems at $z \sim 6$ (G. D. Becker et al. 2009, in preparation). For now, however, we can offer some speculation based on the C IV results alone.

Perhaps the most striking feature of the high-redshift C IV evolution is how rapidly it proceeds at $z > 4.5$. As noted above, both the integrated comoving mass density ($\Omega_{C\,IV}$) and the column density distribution ($f(N_{C\,IV})$) remain nearly invariant over $2 \lesssim z \lesssim 4.5$. Our redshift coverage extends down to $z = 5.3$, which means that much of the buildup of C IV, at least for the weaker systems, must happen over an interval $\Delta z \lesssim 1$, or $\Delta t \lesssim 300$ Myr. By comparison, neither the comoving star-formation rate density nor the stellar mass density is likely to increase by more than a factor of 3 from $z \sim 5.3$–6 to $z \sim 4.5$ (Bouwens et al. 2006; Yan et al. 2006; Stark et al. 2007; Eyles et al. 2007).

Oppenheimer & Davé (2006, 2008) have recently addressed the observed C IV evolution using numerical simulations of large-scale structure, including various prescriptions for feedback from galactic winds. They find that a relatively constant $\Omega_{C\,IV}$ and $f(N_{C\,IV})$ over $z \sim 2$–5 can be produced by a steadily increasing IGM metallicity offset by a declining C IV/C ratio due to energy input from winds. Significantly, they find that in order to produce enough systems at $z = 3.0$–4.5, the metals must largely be in place by $z = 4.5$–6.0. Their best-fitting model ("vzw" from Oppenheimer & Davé 2006) uses momentum-driven winds whose strength is tuned to strike the best balance between metal enrichment and energy injection. Convolving their $f(N_{C\,IV})$ from this model at $z \sim 4.5$–6.0 with our completeness, and making a first-order correction based on the fact that their $\Omega_{C\,IV}$ declines by roughly a factor of 2 from $z \sim 4.5$–5.3 to $z \sim 5.3$–6.0, we would expect to see ~13 C IV systems in our data. This is strongly excluded, which suggests that the mean metallicity and/or the ionization fraction of C IV at $z > 5.3$ must be evolving significantly more rapidly than in their simulations. In order to explain the observed increase in the number density of C IV systems through changes in the mean metallicity alone, the metallicity would have to be lower at $z \sim 6$ and increase roughly twice as fast up to $z \sim 4.5$ as their simulations predict. There is no apparent reason, however, why the rate of enrichment should then decrease at $z < 4.5$. This accelerated enrichment scenario may therefore be difficult to reconcile with the observed plateau in $\Omega_{C\,IV}$ over $z \sim 2$–4.5. Instead, changes in the ionization fraction may provide a more natural explanation for the evolution in C IV at $z > 4.5$.

An important feature of the Oppenheimer & Davé (2006) results is that C IV traces increasingly smaller overdensities at higher redshifts (see also Simcoe 2006). The observed dropoff in C IV may therefore indicate that most of the metals at $z > 5.3$ are confined to overdensities greater than those where C IV is a sensitive tracer of metallicity ($-1 \lesssim \log \rho/\bar{\rho} \lesssim 1$ at $z \sim 5.5$; Oppenheimer & Davé 2006). The gradient in metallicity with density might have to be fairly steep in order to suddenly recover the observed number density of C IV systems at $z \sim 4.5$ by shifting the C IV "window" to larger overdensities. If the metal-enriched regions are marginally self-shielded at $z > 5.3$, however, then a moderate increase in the UV background may be sufficient to produce a large increase in the number of C IV systems over a relatively small Δz. A hardening of the UV background could also produce an increase in the C IV/C ratio. Madau & Haardt (2009) have recently pointed out that absorption in the Lyman series of He II in the IGM can substantially decrease the intensity of the UV background at energies near the ionization potential of C III (3.5 Ryd). If the volume filling fraction of He II is significantly smaller at $z \sim 4.5$ than at $z > 5.3$, as would be expected for an extended He II reionization process (e.g., Bolton et al. 2009; McQuinn et al. 2009), then the shape of the UV background may be more favorable to C IV at $z \sim 4.5$ than at $z > 5.3$.

Given the strong C IV systems identified by Simcoe (2006) and Ryan-Weber et al. (2006), it is especially surprising that we did not detect any weak systems. The two C IV systems toward SDSS J1030+0524 are marginally consistent with a power-law column density distribution under the constraints provided by our data. For example, for our 95% upper limit on the normalization of $f(N_{C\,IV})$ for $\alpha = 1.8$ (Figure 6), there is a 6% chance that a single sight line spanning $\Delta X = 3.1$ would contain at least two systems with $13.8 < \log N_{C\,IV} < 15.0$. Among the six sight lines included here and in the previous studies, however, there would be a 30% chance that at least one sight line would contain two or more strong systems. This increases to 63% for $\alpha = 1.0$, but in either case the lack of detections along our four sight

lines would have been highly unlucky. If the strong C IV systems toward SDSS J1030+0524 are truly intergalactic, then there may be large-scale enrichment and/or ionization fluctuations in the $z \sim 6$ IGM.

Alternatively, the strong C IV systems may simply trace rare sites of active star formation. As noted by Simcoe (2006), there is good evidence that strong C IV systems at lower redshifts are closely associated with actively star-forming galaxies (Adelberger et al. 2003, 2005; Simcoe et al. 2006). Even if metals are largely absent from the general $z \sim 6$ IGM, or in lower ionization states, C IV systems may arise near vigorously star-forming galaxies, where the metallicity and the local ionizing background are enhanced. There is tentative evidence that this is the case from a search for $z \sim 6$ Lyman break galaxies carried out by Kim et al. (2009), who used *Hubble Space Telescope* (*HST*)/ACS to search for *i*-dropouts in the fields of five $z \sim 6$ QSO. Compared to the GOODS field, they find overdensities in only two fields, with the strongest overdensity toward SDSS J1030+0524 (first reported by Stiavelli et al. 2005). The *i*-dropouts in that field appear spatially clustered, and their $i-z$ colors are consistent with star-forming galaxies at $z \sim 5.8$ (Bouwens et al. 2006). This suggests that the two strong C IV absorbers seen toward SDSS J1030+0524 may be associated with outflows from UV-bright galaxies in a foreground filament.

In contrast, an underdensity of *i*-dropouts is seen toward SDSS J1148+5251, whose sight lines does not contain any $z > 5.3$ C IV absorbers. This sight line is known to contain multiple $z \sim 6$ O I systems, however (Becker et al. 2006). The presence of metals in a low-ionization state, combined with the lack of UV-bright galaxies, suggests that this sight line was enriched at $z > 6$, but lacks a sufficient amount of ongoing star formation to keep the enriched gas highly ionized. We will return to this point in a subsequent paper. Finally, we note that the SDSS J0836+0054 field contains an overdensity of *i*-dropouts (Zheng et al. 2006) yet does not show any C IV or O I (Becker et al. 2006). If these galaxies are embedded in a protocluster surrounding the radio-loud QSO, then hard UV photons from the QSO itself may be over-ionizing any metal-enriched gas such that it does not appear as C IV. Spectroscopic follow-up of the *i*-dropouts in QSO fields will help determine whether these scenarios are correct.

6. CONCLUSIONS

We have presented a survey for C IV at $z = 5.3$–6.0 toward four $z \sim 6$ QSOs using Keck/NIRSPEC in echelle mode. This is the most sensitive search for C IV at these redshifts to date, yet we find no clear C IV systems in any of our spectra. Based on our completeness estimates and the column density distribution of Songaila (2001), which remains largely invariant over $2 < z < 4.5$, we would have expected to detect roughly 12 systems in the range $13.2 < \log N_{\rm C\,IV} < 15.0$ in the case of no evolution out to $z \sim 6$. Our lack of detections implies that the number density of C IV absorbers to which our data are sensitive declines by at least a factor of ~4.1 (95% confidence) from $z \sim 4.5$.

Our null result places strong constraints on the shape and normalization of the C IV column density distribution at $z = 5.3$–6.0. For a power-law distribution, $f(N_{\rm C\,IV}) \propto N_{\rm C\,IV}^{-\alpha}$, with a slope equal to that measured at $z \sim 3$ ($\alpha \approx 1.8$), the normalization must decline by at least a factor of 4.1 (95%). The distribution may also flatten or steepen, but only a narrow range of normalizations is allowed for each α by our data and the fact that at least two strong ($\log N_{\rm C\,IV} > 13.8$) systems are seen in the two previously studied sight lines (Simcoe 2006; Ryan-Weber et al. 2006, and confirmed herein). Our limits on $\Omega_{\rm C\,IV}$ are less strict due to the fact that the comoving density can be dominated by rare, strong systems. Within the range $13.2 < \log N_{\rm C\,IV} < 15.0$, however, the constraints on $f(N_{\rm C\,IV})$ imply that $\Omega_{\rm C\,IV}$ must decline by at least a factor of 2 from $z \sim 2$–4.5 to $z = 5.3$–6.0 (see also Ryan-Weber et al. 2009). The fact that $f(N_{\rm C\,IV})$ and $\Omega_{\rm C\,IV}$ are relatively constant at $z \lesssim 4.5$ further means that most of the buildup of C IV in the IGM must occur over an interval $\Delta z \lesssim 1$, or $\Delta t \lesssim 300$ Myr.

The rapidness with which C IV in the IGM increases between $z \sim 5.3$ and $z \sim 4.5$ suggests that ionization effects may be playing an important role. That is, a significant fraction of intergalactic metals we see as C IV at $z \sim 4.5$ may already be in place at $z > 5.3$, but in a lower ionization state. This may especially be true if the metals are confined to relatively high overdensities (e.g., Oppenheimer & Davé 2006). An increase in the C IV/C ratio could result from an increase in the intensity or a hardening of the UV background, or as galactic outflows propagate into lower density regions. The rapid buildup of C IV systems might also be explained if the mean IGM metallicity increases roughly twice as fast at high redshifts as is seen in the Oppenheimer & Davé (2006, 2008) simulations, though an accelerated enrichment scenario may be difficult to reconcile with the plateau in $\Omega_{\rm C\,IV}$ at $z < 4.5$. Measuring the abundance of metals in lower ionization states will help to disentangle the effects of ionization and enrichment. We will do this in a subsequent work.

The contrast between our lack of detections along four sight lines and the presence of two strong C IV absorbers toward SDSS J1030+0524 suggests that there may be large-scale variations in IGM enrichment and/or in the ionization state of the metal-enriched gas. Alternatively, the strong C IV systems may be associated with rare, UV-bright star-forming galaxies, in which case the enhancement of C IV would be a local effect. We are currently planning follow-up observations of SDSS J1030+0524 to look for weak C IV systems. The presence of additional C IV would more strongly indicate that this sight line is either more enriched or more highly ionized than those in our current sample. In addition, spectroscopic follow-up of the *i*-dropouts in field of SDSS J1030+0524 (Stiavelli et al. 2005; Kim et al. 2009) may clarify whether the C IV absorbers are closely associated with UV-bright galaxies.

Finally, we note that the decline of C IV at $z > 5.3$ poses an interesting challenge to the use of low-ionization metal lines as tracers of reionization. Unless additional metals are lurking in intermediate ionization states, no "O I forest" may appear at $z \gtrsim 6$ simply because the IGM is not sufficiently enriched at early times. On the other hand, the detection of a significant number of neutral metal absorption systems at $z \sim 6$ could have a double significance: that the IGM is at least partially metal-enriched by that redshift, and that pockets of the IGM were not permanently ionized until well after the early reionization epoch favored by CMB studies. This will be the focus of a following paper.

The authors thank Emma Ryan-Weber and Max Pettini for many stimulating conversations over the course of this work. We also thank Martin Haehnelt, Bob Carswell, and Rob Simcoe for providing comments on the first draft of this paper, as well as the anonymous referee for several helpful suggestions. The authors wish to recognize the very significant cultural role that the summit of Mauna Kea has always had within the

indigenous Hawaiian community. We are most fortunate to have the opportunity to conduct observations from this mountain. G.B. was supported by the Kavli Institute for Cosmology at the Institute of Astronomy in Cambridge. M.R. was supported by the National Science Foundation through grant AST-0506845. W.S. was supported through grant AST-0606868.

REFERENCES

Adelberger, K. L., Shapley, A. E., Steidel, C. C., Pettini, M., Erb, D. K., & Reddy, N. A. 2005, ApJ, 629, 636
Adelberger, K. L., Steidel, C. C., Shapley, A. E., & Pettini, M. 2003, ApJ, 584, 45
Aguirre, A., Schaye, J., Kim, T.-S., Theuns, T., Rauch, M., & Sargent, W. L. W. 2004, ApJ, 602, 38
Becker, R. H., et al. 2001, AJ, 122, 2850
Becker, G. D., Rauch, M., & Sargent, W. L. W. 2007, ApJ, 662, 72
Becker, G. D., Sargent, W. L. W., Rauch, M., & Simcoe, R. A. 2006, ApJ, 640, 69
Boksenberg, A., Sargent, W. L. W., & Rauch, M. 2003, arXiv:astro-ph/0307557
Bolton, J. S., Oh, S. P., & Furlanetto, S. R. 2009, MNRAS, in press (arXiv:0807.2447)
Bouwens, R. J., Illingworth, G. D., Blakeslee, J. P., & Franx, M. 2006, ApJ, 653, 53
Cowie, L. L., Songaila, A., Kim, T.-S., & Hu, E. M. 1995, AJ, 109, 1522
Dijkstra, M., Wyithe, J. S. B., & Haiman, Z. 2007, MNRAS, 379, 253
Dunkley, J., et al. 2009, ApJS, 180, 306
Ellison, S. L., Lewis, G. F., Pettini, M., Chaffee, F. H., & Irwin, M. J. 1999, ApJ, 520, 456
Eyles, L. P., Bunker, A. J., Ellis, R. S., Lacy, M., Stanway, E. R., Stark, D. P., & Chiu, K. 2007, MNRAS, 374, 910
Fan, X., Narayanan, V. K., Strauss, M. A., White, R. L., Becker, R. H., Pentericci, L., & Rix, H.-W. 2002, AJ, 123, 1247
Fan, X., et al. 2006, AJ, 132, 117
Furlanetto, S. R., Zaldarriaga, M., & Hernquist, L. 2006, MNRAS, 365, 1012
Gehrels, N. 1986, ApJ, 303, 336
Gnedin, N. Y., & Fan, X. 2006, ApJ, 648, 1
Haiman, Z., & Cen, R. 2005, ApJ, 623, 627
Hinkle, K. H., Wallace, L., & Livingston, W. 2003, BAAS, 35, 1260
Horne, K. 1986, PASP, 98, 609
Hu, E. M., & Cowie, L. L. 2006, Nature, 440, 1145
Lidz, A., Oh, S. P., & Furlanetto, S. R. 2006, ApJ, 639, L47
Kashikawa, N., et al. 2006, ApJ, 648, 7
Kelson, D. D. 2003, PASP, 115, 688
Kim, S., et al. 2009, ApJ, 695, 809
Komatsu, E., et al. 2009, ApJS, 180, 330
Madau, P., & Haardt, F. 2009, ApJ, 693, L100
Malhotra, S., & Rhoads, J. E. 2004, ApJ, 617, L5
Malhotra, S., & Rhoads, J. E. 2006, ApJ, 647, L95
McLean, I. S., et al. 1998, Proc. SPIE, 3354, 566
McQuinn, M., Lidz, A., Zaldarriaga, M., Hernquist, L., Hopkins, P. F., Dutta, S., & Faucher-Giguére, C.-A. 2009, ApJ, 694, 842
Meyer, D. M., & York, D. G. 1987, ApJ, 315, L5
Nestor, D., Hamann, F., & Hidalgo, P. R. 2008, MNRAS, 386, 2055
Oh, S. P. 2002, MNRAS, 336, 1021
Oh, S. P., & Furlanetto, S. R. 2005, ApJ, 620, L9
Oppenheimer, B. D., & Davé, R. 2006, MNRAS, 373, 1265
Oppenheimer, B. D., & Davé, R. 2008, MNRAS, 387, 577
Petitjean, P., & Bergeron, J. 1994, A&A, 283, 759
Pettini, M., Madau, P., Bolte, M., Prochaska, J. X., Ellison, S. L., & Fan, X. 2003, ApJ, 594, 695
Rauch, M., Sargent, W. L. W., Womble, D. S., & Barlow, T. A. 1996, ApJ, 467, L5
Ryan-Weber, E. V., Pettini, M., & Madau, P. 2006, MNRAS, 371, L78
Ryan-Weber, E. V., Pettini, M., Madau, P., & Zych, B. J. 2009, MNRAS, submitted (arXiv:0902.1991)
Santos, M. R. 2004, MNRAS, 349, 1137
Sargent, W. L. W., Boksenberg, A., & Steidel, C. C. 1988, ApJS, 68, 539
Scannapieco, E., Pichon, C., Aracil, B., Petitjean, P., Thacker, R. J., Pogosyan, D., Bergeron, J., & Couchman, H. M. P. 2006, MNRAS, 365, 615
Schaye, J., Aguirre, A., Kim, T.-S., Theuns, T., Rauch, M., & Sargent, W. L. W. 2003, ApJ, 596, 768
Simcoe, R. A. 2006, ApJ, 653, 977
Simcoe, R. A., Sargent, W. L. W., & Rauch, M. 2004, ApJ, 606, 92
Simcoe, R. A., Sargent, W. L. W., Rauch, M., & Becker, G. 2006, ApJ, 637, 648
Songaila, A. 2001, ApJ, 561, L153
Songaila, A. 2004, AJ, 127, 2598
Songaila, A. 2005, AJ, 130, 1996
Stark, D. P., Bunker, A. J., Ellis, R. S., Eyles, L. P., & Lacy, M. 2007, ApJ, 659, 84
Stiavelli, M., et al. 2005, ApJ, 622, L1
Vestergaard, M. 2003, ApJ, 599, 116
Vogt, S. S., et al. 1994, Proc. SPIE, 2198, 362
White, R. L., Becker, R. H., Fan, X., & Strauss, M. A. 2003, AJ, 126, 1
Wyithe, J. S. B., & Loeb, A. 2005, ApJ, 625, 1
Yan, H., Dickinson, M., Giavalisco, M., Stern, D., Eisenhardt, P. R. M., & Ferguson, H. C. 2006, ApJ, 651, 24
Zheng, W., et al. 2006, ApJ, 640, 574